Canadian Chemical Transactions

ISSN 2291-6458 (Print), ISSN 2291-6466 (Online)
Year 2014 | Volume 2 | Issue 2 | Page 175-189

Research Article

DOI:10.13179/canchemtrans.2014.02.02.0092

Analysis of Molecular Structures, Spectroscopic Properties (FT-IR, Micro-Raman and UV-vis.) and Quantum Chemical Calculations of Free and Ligand Dimethyl Phenylphosphonite in Cd(II) Halide Complex

Semiha Bahçeli[1,*] and Halil Gökce[2]

[1]*Department of Physics, Faculty of Arts and Science, Süleyman Demirel University, East Campus, 32260, Isparta, TURKEY*
[2]*Vocational High School of Health Services, Giresun University, Güre Campus, 28200, Giresun, TURKEY*

[*]*Corresponding Author, E-mail: s.bahceli.80@gmail.com*

Received: *January 22, 2014* ***Revised:*** *February 17, 2014* ***Accepted:*** *February 18, 2014* ***Published:*** *February 20, 2014*

Abstract: In this study the molecular geometries, experimental vibrational and electronic absorption spectra and quantum chemical calculations of free dimethyl phenylphosphonite, (C8H11PO2), (with synonym, dimethoxyphenylphosphine or phenyldimethoxyphosphine) (Abbreviated as DMPP) and its [Cd(DMPP)].Cl2.H2O metal halide complex have been investigated by using elemental analysis, FT-IR, micro-Raman and UV-vis spectroscopies. The conformational analysis of free DMPP, the structures, vibrational wavenumbers and HOMO-LUMO and MEP analyses of the mentioned compounds have been computed by using DFT/B3LYP calculation method with 6-311++G(d,p) basis set for free DMMP molecule and DFT/B3LYP and DFT/M06-L methods with LanL2DZ basis set for [Cd(DMPP)].Cl2.H2O metal halide complex, in the ground state. The comparison of the observed fundamental vibrational frequencies with calculated results indicates that DFT/M06-L method is superior to the scaled DFT/B3LYP approach for the vibrational modes related to the metal atom of [Cd(DMPP)].Cl2.H2O metal halide complex.

Keywords: Dimethyl Phenyl Phosphonite; Vibrational Spectroscopy; Electronic Absorption Spectroscopy; Transition Metal; Density Functioal Theory

1. INTRODUCTION

In the past, the hypodermic solution of sodium dimethyl phenylphosphonite (DMPP) and its methiodide derivative have been studied by Ruggieri in a medicinal research [1]. Later, some organic phosphorous compounds containing phosphonite and its derivatives were introduced to the chemical industry [2,3]. The donor ligand and coordinating properties of dimethyl phenylphosphonite molecule

ISSN 2291-6458 (Print), ISSN 2291-6466 (Online)
Year 2014 | Volume 2 | Issue 2 | Page 175-189

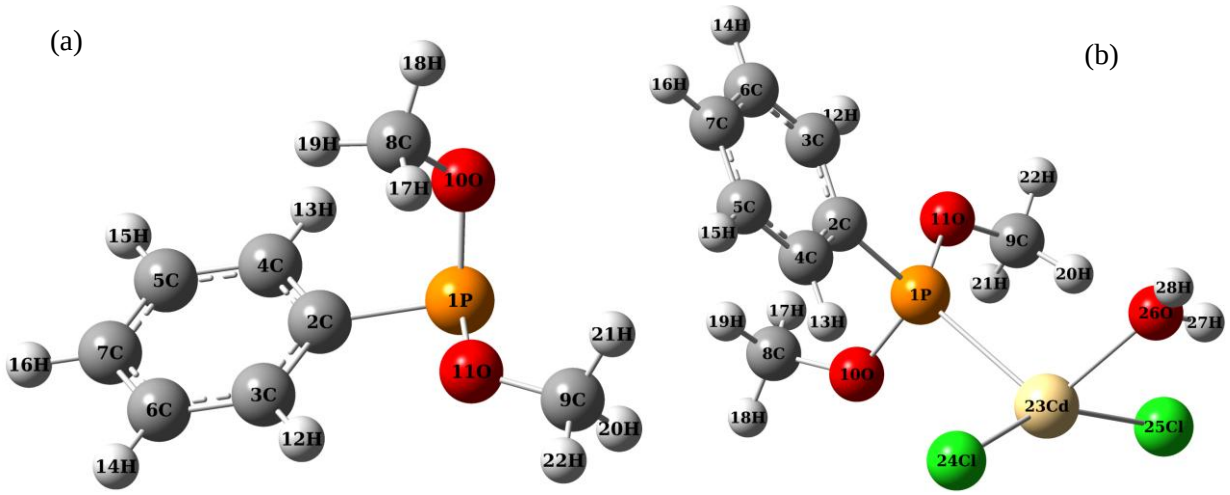

Figure 1. The optimized molecular geometries of free DMPP molecule and $[Cd(C_8H_{11}PO_2)].Cl_2$. H_2O complex at the B3LYP/6-311++G(d,p) and BLYP/ and M06-L/LanL2DZ levels, respectively.

with various metals have attracted a great interest in chemistry field. In this framework, IR and ^{1}H NMR spectra of the Cr, Mo and W metal complexes of DMPP have been presented by Jenkins *et al.* [4]. Likewise the syntheses and ^{1}H NMR spectra of the copper, silver and gold metal complexes including dimethyl phenylphosphonite have been investigated by Couch and Robinson [5]. Also, the synthesis and NMR investigation of the ruthenium complex of DMPP have been studied by Sime and Stephenson [6]. Likewise, the methyl methylphosphinate complexes of the first-row transition metals were synthesized and investigated using IR and UV spectroscopies by Mikulski *et al.* [7]. Furthermore, the various compounds containing the derivatives of dimethyl phenylphosphonite have been investigated as a ligand in some metal halide complexes [8-12]. Very recently, anomalous reaction of ethylbromofluoro and difluoro acetates with dialkylphosphonites has been reported by Durst *et al.* [13]. Meanwhile, the crystallographic structures of Pd(II) and Pt(II) metal halides of dimethyl phenylphosphonite have been verified by Slawin *et al.* [14,15].

To our best knowledge, there are no any further studies on both free and ligand dimethyl phenylphosphonite molecule in the title compound by using DFT calculation method, FT-IR, micro-Raman and UV-vis. spectroscopies in the literature. At the present work, our aim is to report the results of the observed FT-IR, micro-Raman and electronic absorption spectra and calculated vibrational frequency values of free and ligand DMPP molecule in the $[Cd(DMPP)].Cl_2.H_2O$ complex at DFT/B3LYP with 6-311++G(d,p) and DFT/ B3LYP and M06-L methods with LanL2DZ basis set, respectively.

2. EXPERİMENTAL METHODS

2.1. Materials and Sample Preparation

Dimethyl phenylphosphonite (97%, Sigma-Aldrich) and $CdCl_2$ (99%, Fluka) used in this work were obtained from commercial sources and were used without any purification. First, 1 mmol of DMPP was added to 1 mmol of $CdCl_2$ dissolved in 5 ml of water. After the mixture was stirring during 24h, the obtained precipitate was filtered, washed twice with ethylalcohol and dried at room temperature.

2.2. Experimental Techniques and Elemental Analysis

IR spectra of dimethyl phenylphosphonite and its metal halide complex were recorded at room temperature on a Perkin Elmer Spectrum One FT–IR (Fourier Transform Infrared) Spectrometer with a resolution of 4 cm^{-1} in the transmission mode. The sample was prepared by dropping title liquid onto the

ISSN 2291-6458 (Print), ISSN 2291-6466 (Online)
Year 2014 | Volume 2 | Issue 2 | Page 175-189

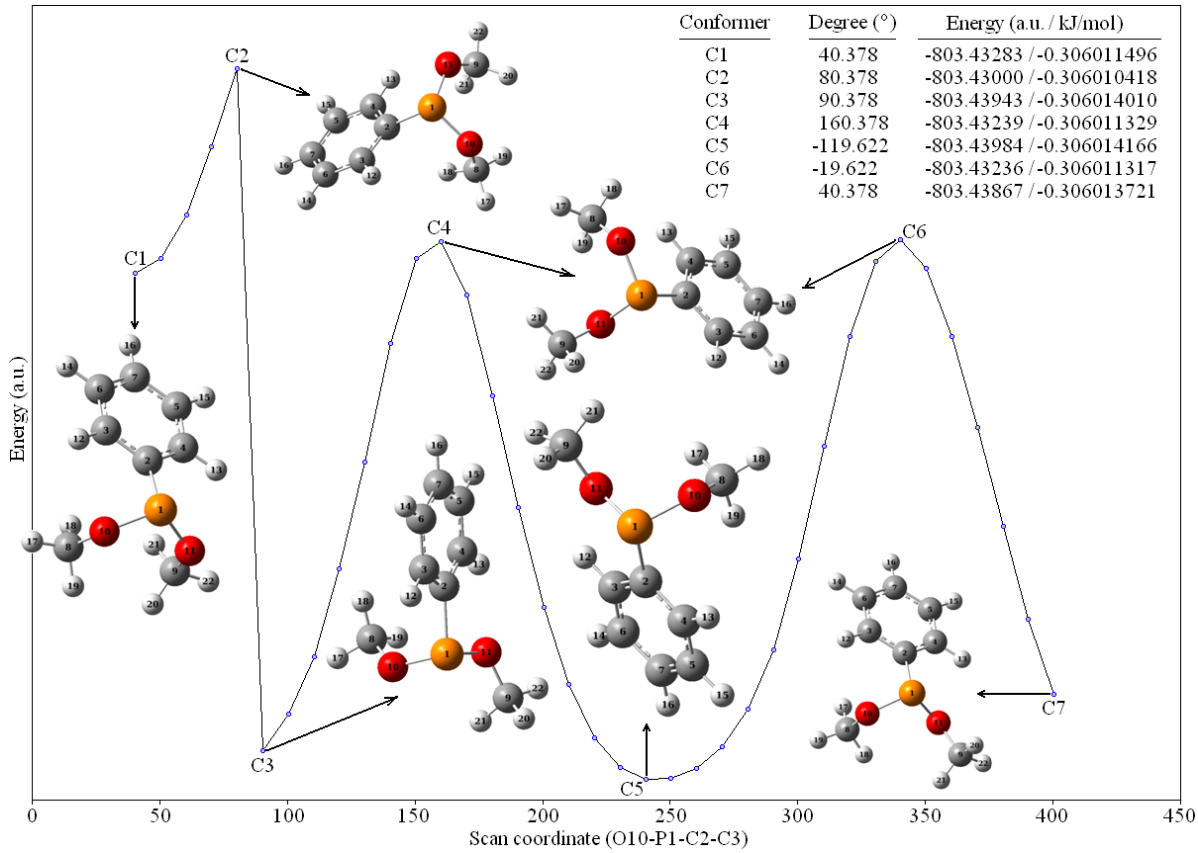

Figure 2. Conformational analysis of free DMPP at the B3LYP/6-311++G(d,p) level.

KBr pellet and introduced into an IR cell equipped with KBr window. On the other hand, the micro-Raman (μ–Ra) spectra of the mentioned compounds were recorded by using a Jasco NRS–3100 micro–Raman Spectrophotometer (1800 lines/mm grating and high sensitivity cooled CCD) at room temperature in the region 100–4000 cm^{-1}. The spectrometer was calibrated with the silicon phonon mode at 520 cm^{-1} and microscope objective 100x was used. The 785 nm lines of diode laser was used for excitation. The exposure time was taken as 15 s and 10 scans were accumulated. The ultraviolet visible spectrum of the title compounds were recorded by using a PG Instrument T80+ Ultraviolet Spectrophotometer at room temperature. The ultraviolet visible spectrum of the mentioned compound solved in dimethylformamide were recorded with a spectral bandwidth of 2 nm in a quartz cell 1cm path length.

The prepared $[Cd(C_8H_{11}PO_2)].Cl_2.H_2O$ metal halide complex was analysed by using a LECO CHNS 932 model analyzer for C and H with the following results (found% / calculated%) C: 24.52/25.87; H: 2.68/3.53; for which is tetrahedral.

3. COMPUTATIONAL DETAILS

In this study, all calculations were carried out with the Gaussian 09 program and GaussView 5 molecular visualization program [16,17].

The molecular structure and vibrational computations of dimethyl phenylphosphine molecule was calculated by using Becke-3-Lee Yang Parr (B3LYP) [18,19] density functional theory method with 6-311++G(d,p) basis set in ground state. The positive values of all calculated vibrational wavenumbers show that the optimized molecular structure is stable. However, the wavenumber values computed at these levels contain the well-known systematic errors [20]. In order to prevent the well-known systemetic

ISSN 2291-6458 (Print), ISSN 2291-6466 (Online)
Year 2014 | Volume 2 | Issue 2 | Page 175-189

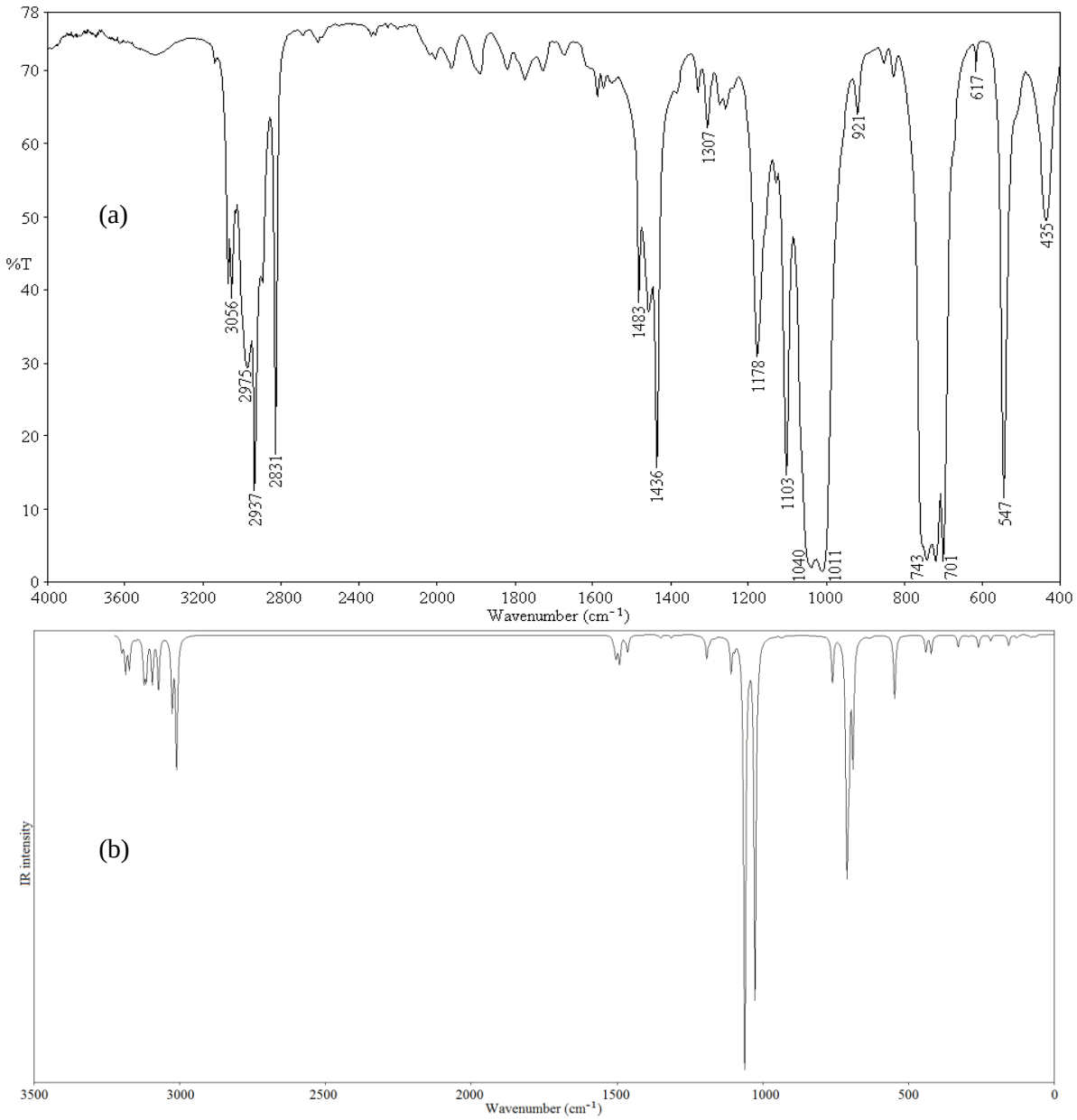

Figure 3. (a) Experimental and (b) Calculated IR spectra at the B3LYP/6-311++G(d,p) level of theory of free DMPP.

errors the computed vibrational wavenumbers were scaled as 0.983 for frequencies less than 1700 cm^{-1} and 0.958 for frequencies higher than 1700 cm^{-1} at B3LYP/6–311++G(d,p) basis set [21,22]. The molecular structures and vibrational calculations of the [Cd(DMPP)].Cl_2.H_2O metal halide complex were computed using two different methods which are the standard B3LYP and M06-L local functional of the density functional theory by comparing their performance for application in complexes including transition metals [23,24]. For the LanL2DZ basis set used in the mentioned calculation methods the scaling factor was taken as 0.9612 [25]. The assignments of fundamental vibrational modes of the title molecules were performed on the basis of total energy distribution (TED) analysis by using VEDA 4 program [26].

ISSN 2291-6458 (Print), ISSN 2291-6466 (Online)
Year 2014 | Volume 2 | Issue 2 | Page 175-189

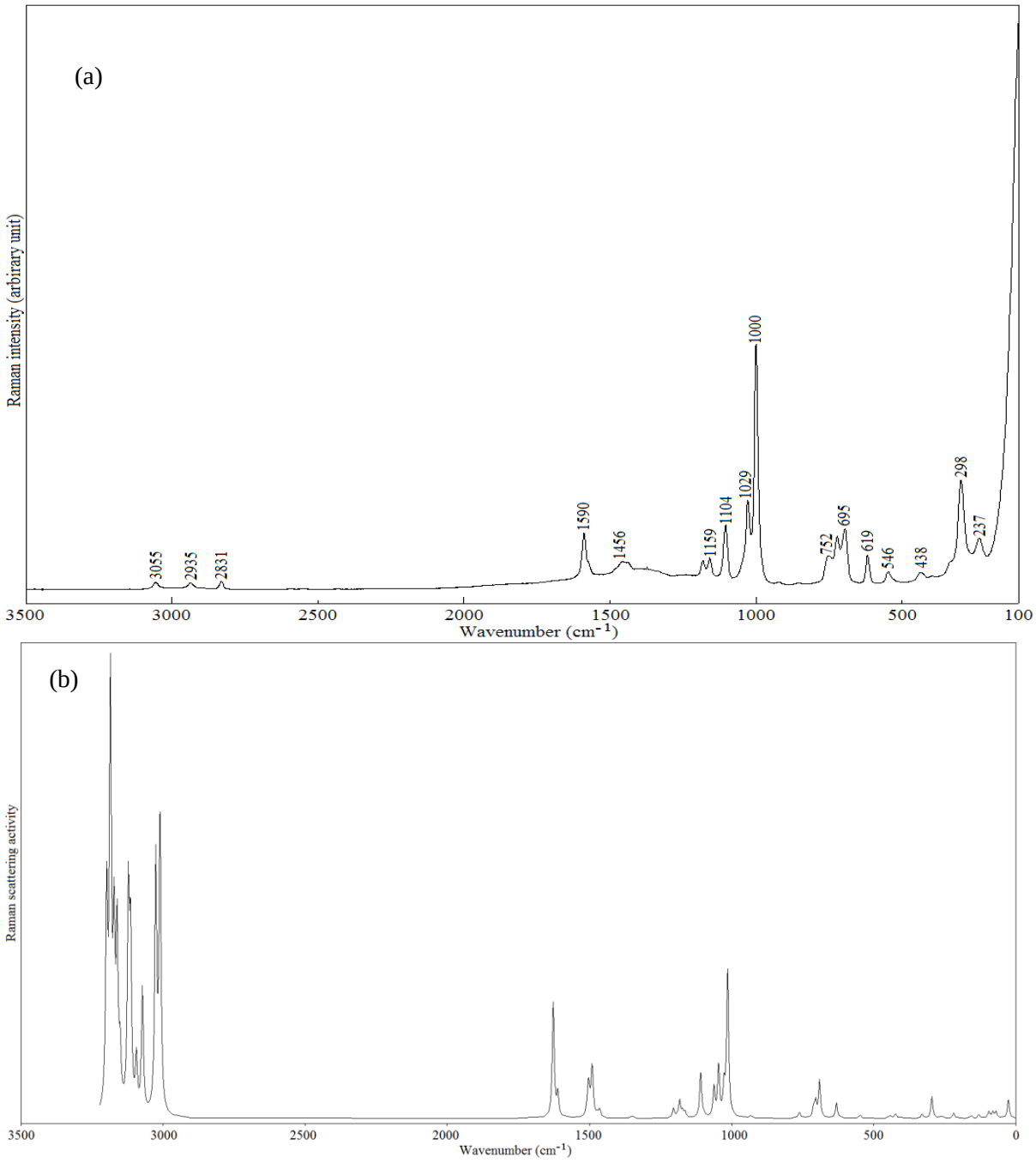

Figure 4. (a) Experimental and (b) Calculated Raman spectra at the B3LYP/6-311++G(d,p) level of theory of free DMPP

The HOMO-LUMO and molecular electrostatic potentials (MEP) calculations of the title compounds were performed using DFT/B3LYP method with 6-311++G(d,p) basis set for free DMPP and DFT/B3LYP and M06-L methods with LanL2DZ basis sets for its metal halide complex. Furthermore, the orbital shapes (HOMO-LUMO) and molecular electrostatic potential (MEP) of the mentioned free molecule and metal complex in 3-dimensional (3D) were plotted by using at B3LYP/6-311++G(d,p) and B3LYP/ and M06-L/ LanL2DZ levels, respectively, in GaussView 5 program.

ISSN 2291-6458 (Print), ISSN 2291-6466 (Online)
Year 2014 | Volume 2 | Issue 2 | Page 175-189

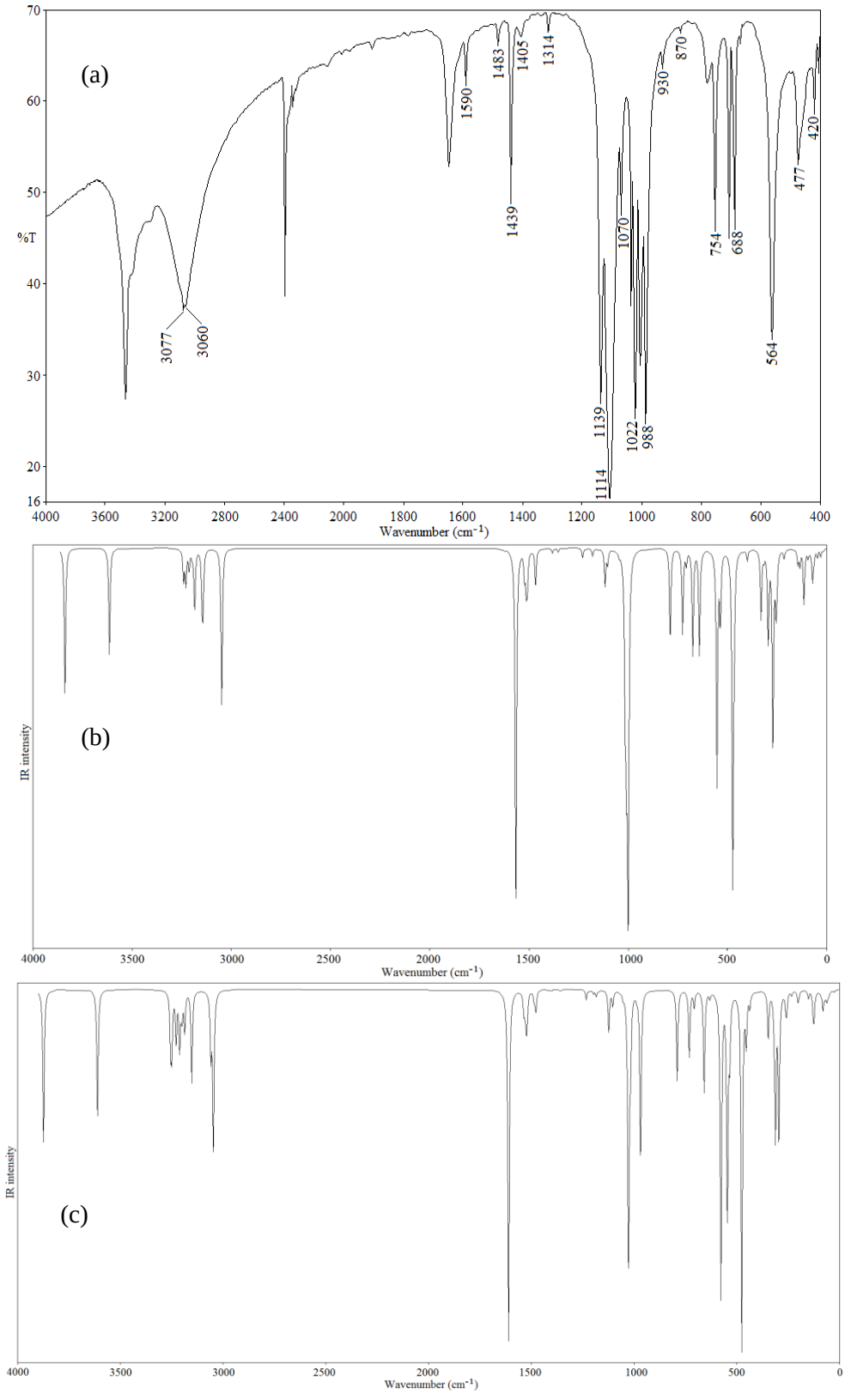

Figure 5. (a) Experimental, (b) Calculated IR spectra at the B3LYP/LanL2DZ level and (c) at the M06-L/LanL2DZ level of theory of $Cd(DMPP)Cl_2.H_2O$ complex

ISSN 2291-6458 (Print), ISSN 2291-6466 (Online)
Year 2014 | Volume 2 | Issue 2 | Page 175-189

The Raman activities (S_i) calculated by using Gaussian 09 program have been converted to relative Raman intensities (I_i) using the following relationship,

$$I_i = \frac{f(\upsilon_0 - \upsilon_i)^4 S_i}{\upsilon_i[1-\exp(-hc\upsilon_i / kT)]},$$

where υ_0 (cm^{-1}) is the exciting frequency, υ_i is the vibrational wavenumber of the i^{th} normal mode, *h*, *c*, and *k* are well–known universal constants and *f* is the suitably chosen common scaling factor for all the peak intensities [27,28].

4. RESULTS AND DİSCUSSİON

4.1. Molecular Structures and Vibrational Frequencies

The optimized molecular structure obtained at the B3LYP/6-311++G(d,p) level of free dimethyl phenylphosphonite molecule and at the B3LYP/ and M06-L/LanL2DZ levels of its metal Cd(II) halide complex are given in Figure 1 (a) and (b), respectively. Table S1 (Supporting Information) shows only the calculated geometric parameters of the mentioned compounds since dimethyl phenylphosphonite molecule is liquid and the crystallographic structures of the mentioned metal complex is not available in the literature. By considering Table S1, for free DMPP molecule the P1-C2 bond length between the phenyl ring and dimethoxyphosphine group was found as 1.851 Å while the P1-O10 and P1-O11 bond lengths in dimethoxyphosphine group were calculated as 1.659 Å and 1.673 Å, respectively, at the B3LYP/6-311++G(d,p) level. Similarly the C-C and C- H bond length values in phenyl ring were found at the interval 1.393-1.402 Å and 1.083-1.086 Å, respectively, while the C-H bond length values in methyl groups are calculated at the interval 1.090-1.095 Å. Furthermore the C8-O10 and C9-O11 bond lengths in methoxyphosphine group were found as 1.436 Å and 1.432 Å. Likewise, the calculated bond angles and some selected dihedral angles of free DMPP molecule at the B3LYP/6-311++G(d,p) level are presented in Table S1.

However the eventual presence of different conformations of free DMPP molecule should be considered. In this framework the potential energy surfaces (PES) scan was carried out around the C2-P1 axis by changing of the O10-P1-C2-C3 torsion angle at 10° steps from 0° to 360°. Figure 2 indicates the possible conformations of the mentioned molecule with their calculated energy values. However, although the C4 and C6 conformers have the same energy value the directions of benzene ring and P-OCH_3 group are different for the mentioned conformers. In other words, their rotation angles have different values. Therefore the C5 conformation becomes the most stable state of free DMPP molecule and its energy values was calculated as -803.43984 Hartree at the B3LYP/6-311++G(d,p) level.

On the other hand for the [Cd(DMPP)].Cl_2.H_2O metal halide complex the calculated bond length, bond angle and some selected dihedral angle values at the B3LYP/ and M06-L/LanL2DZ levels are in general found very close each other as seen in Table S1. Therefore by considering Figure 1 (b) and Table S1 the Cd-P bond length was calculated as 2.850 Å and 3.515 Å at the B3LYP/LanL2DZ and M06-L/LanL2DZ levels, respectively. For the P atom coordinated to the cadmium metal, the P-C2, P-O10 and P-O11 bond lengths were computed as 1.865-1.866 Å, 1.735-1831 Å and 1.735-1764 Å at the mentioned levels, respectively. Likewise, the Cd-Cl24 and Cd-Cl25 bond lengths were found as 2.446-2.509 Å and 2.495-2.427 Å at the B3LYP/LanL2DZ and M06-L/LanL2DZ levels, respectively. At the same time, the calculated O10-Cd23 and O11-Cd23 bond lengths in the mentioned complex were found as 3.592 and

ISSN 2291-6458 (Print), ISSN 2291-6466 (Online)
Year 2014 | Volume 2 | Issue 2 | Page 175-189

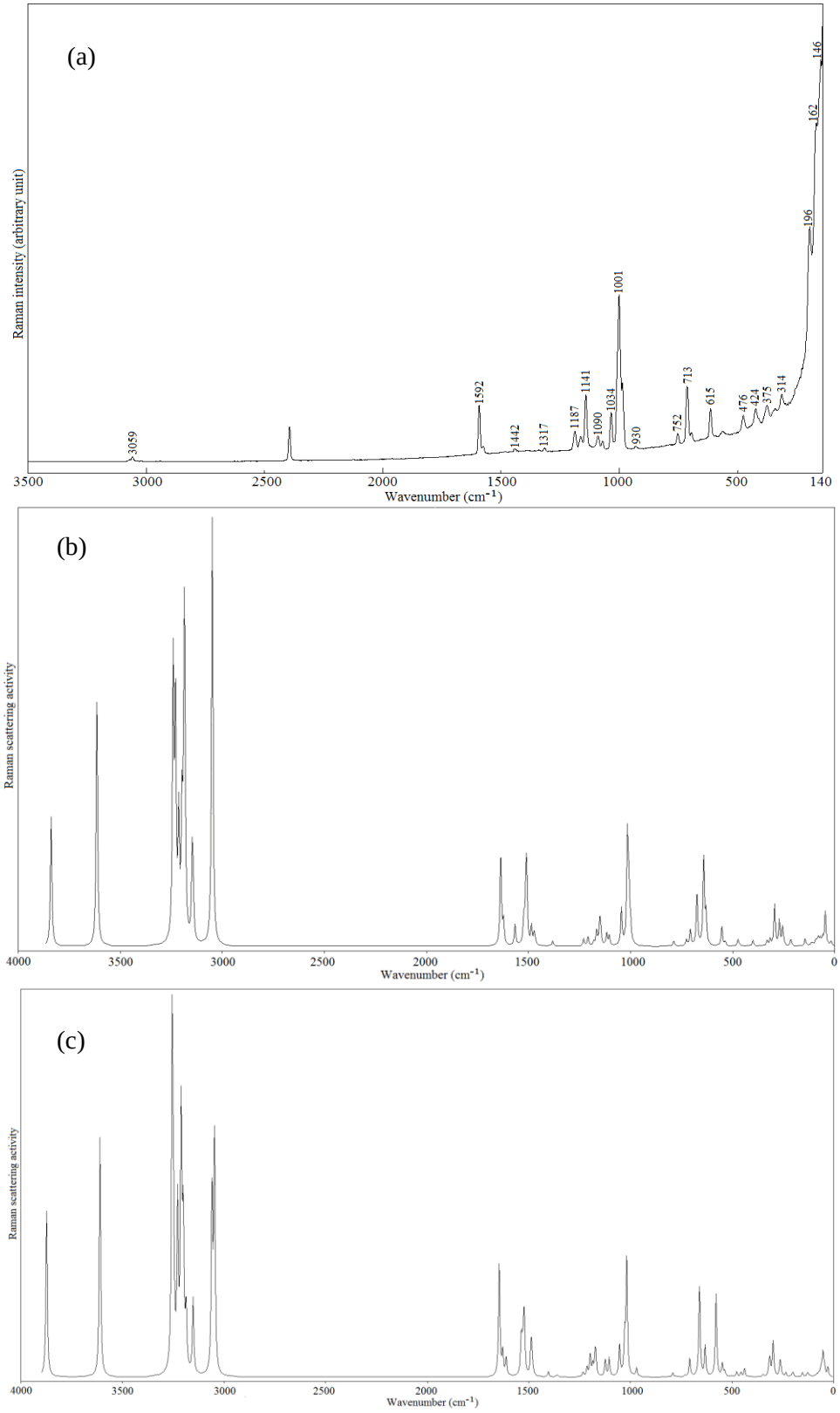

Figure 6. (a) Experimental, (b) Calculated Raman spectra at the B3LYP/LanL2DZ level and (c) at the M06-L/LanL2DZ level of theory of $Cd(DMPP)Cl_2.H_2O$ complex.

ISSN 2291-6458 (Print), ISSN 2291-6466 (Online)
Year 2014 | Volume 2 | Issue 2 | Page 175-189

3.252 Å and 4.077 and 4.789 Å at the B3LYP/ LanL2DZ and M06-L/LanL2DZ levels, respectively. On the other hand, the O10-P-O11 and P-C2-C3 bond angles were calculated as 104.536-97.608^{o} and 122.071-122.494^{o} for Cd^{+2} complex at the mentioned levels, respectively. Furthermore the C2-P-Cd and P-Cd-Cl24 bond angles were computed as 123.141-109.321^{o} and 99.883-72.676^{o} for $[Cd(C_8H_{11}PO_2)].Cl_2.H_2O$ complex at the B3LYP/LanL2DZ and M06-L/LanL2DZ levels, respectively. It is clear that there are some discrepancies in the calculated molecular geometric parameter values of the mentioned metal halide complex at the B3LYP/LanL2DZ and M06-L/LanL2DZ levels, respectively and a comparison cannot be verified between the results calculated at two different levels due to the lack of experimental data.

The experimental and simulated at the B3LYP76-311++G(d,p) level IR and micro-Raman spectra of free DMPP are given in Figure 3(a) and (b) and Figure 4(a) and (b), respectively.

For $[Cd(C_8H_{11}PO_2)].Cl_2.H_2O$ metal halide complex the experimental and simulated at the B3LYP/LanL2DZ and M06-L/LanL2DZ levels IR and micro-Raman spectra are shown in Figure 5(a), (b), and (c) and Figure 6 (a), (b), and (c), respectively. Furthermore the observed and calculated vibrational frequencies, the calculated IR intensities and Raman scattering activities and all vibrational frequency assignments of the compounds under study are listed in Tables S2 and S3 (Supporting Information) for free DMPP and $[Cd(C_8H_{11}PO_2)].Cl_2.H_2O$ complex, respectively.

By considering the states such as negligence of anharmonicity, electron correlation and basis set deficiencies it should be noted that the calculated harmonic vibrational wavenumbers, which were performed in gaseous phase for isolated molecule while the experimental measurements were taken in solid phase of the title molecule, become higher than the observed wavenumbers [20,21]. That is why, the calculated wavenumbers were scaled by scaling factor to compare with observed wavenumbers and at the present work, the scaling factors are taken as 0.983 for frequencies less than 1700 cm^{-1} and 0.958 for frequencies higher than 1700 cm^{-1} at the B3LYP/6–311++G(d,p) level for free DMPP molecule.

From Table S2 and Figures 3 and 4, the vibrational torsion (τHCCC) modes of the phenyl ring of free DMPP molecule can be assigned to the observed peaks at 921 m (IR)-922 vw (R) cm^{-1}, 853 m (IR)-853 vw (R) cm^{-1}, 740 vw (IR)-752 w (R) cm^{-1} and 716 vw (IR)-722 w (R) cm^{-1} while its vibrational out of plane bending γ(CCCC) modes can be attributed to the observed peaks at 1102 s (IR)-1104 m (R) cm^{-1} and 617 m (IR)-619 m (R) cm^{-1}. Likewise the vibrational τ(CCCC) torsion modes for the phenyl ring of free DMPP molecule can be assigned to the observed peaks at 438 w (R) cm^{-1} and 396 vw (R) cm^{-1} [7, 29-30]. On the other hand the P-O stretching vibrational bands of the metoxyphosphine group of free DMPP molecule are observed at 692 vw (IR)-695 m (R) cm^{-1} and the calculated values at the B3LYP/6–311++G(d,p) level were found as 698.65 and 679.04 cm^{-1}, respectively. Likewise, the ν(P-Phenyl) stretching band is observed at 1102 s (IR) -1104 m (R) $cm^{-1}$and its calculated value was found as 1089.93 cm^{-1}. Similarly, the vibrational $\nu(O\text{-}CH_3)$ stretching bands are observed at 1035 vw (IR)-1029 m (R) cm^{-1} and 999 vw (IR)-1000s (R) cm^{-1} and their calculated values were found as 1043.99 and 1009.13 cm^{-1}, respectively. Likewise, the vibrational scissoring (δ_s), the symmetric bending (δ) and rocking (ρ) modes for methyl groups can be attributed to the observed peaks at 1456 w (IR) - 1456 w (R) cm^{-1}, 1435 vs (IR) -1441 w (R) cm^{-1} and 1178 s (IR) – 1183 w (R) cm^{-1}, 1132 m (IR) -1159 w (R) cm^{-1}, respectively. Likewise, the peaks observed at 578 m (IR) - 546 w (R) cm^{-1} can be attributed the vibrational δ(C-O-P) mode [7].

For the vibrational frequency calculations of $[Cd(DMPP)].Cl_2\ H_2O$ metal halide complex at B3LYP/LanL2DZ and M06-L/LanL2DZ levels, the scaling factor was taking as 0.9612 [25]. In this framework by considering Figures 5 (a) and 6 (a), the strong IR band at 2400 cm^{-1} and the micro-Raman band with medium intensity at 2393 cm^{-1} which are not observed in the vibrational spectra of free DMPP

ISSN 2291-6458 (Print), ISSN 2291-6466 (Online)
Year 2014 | Volume 2 | Issue 2 | Page 175-189

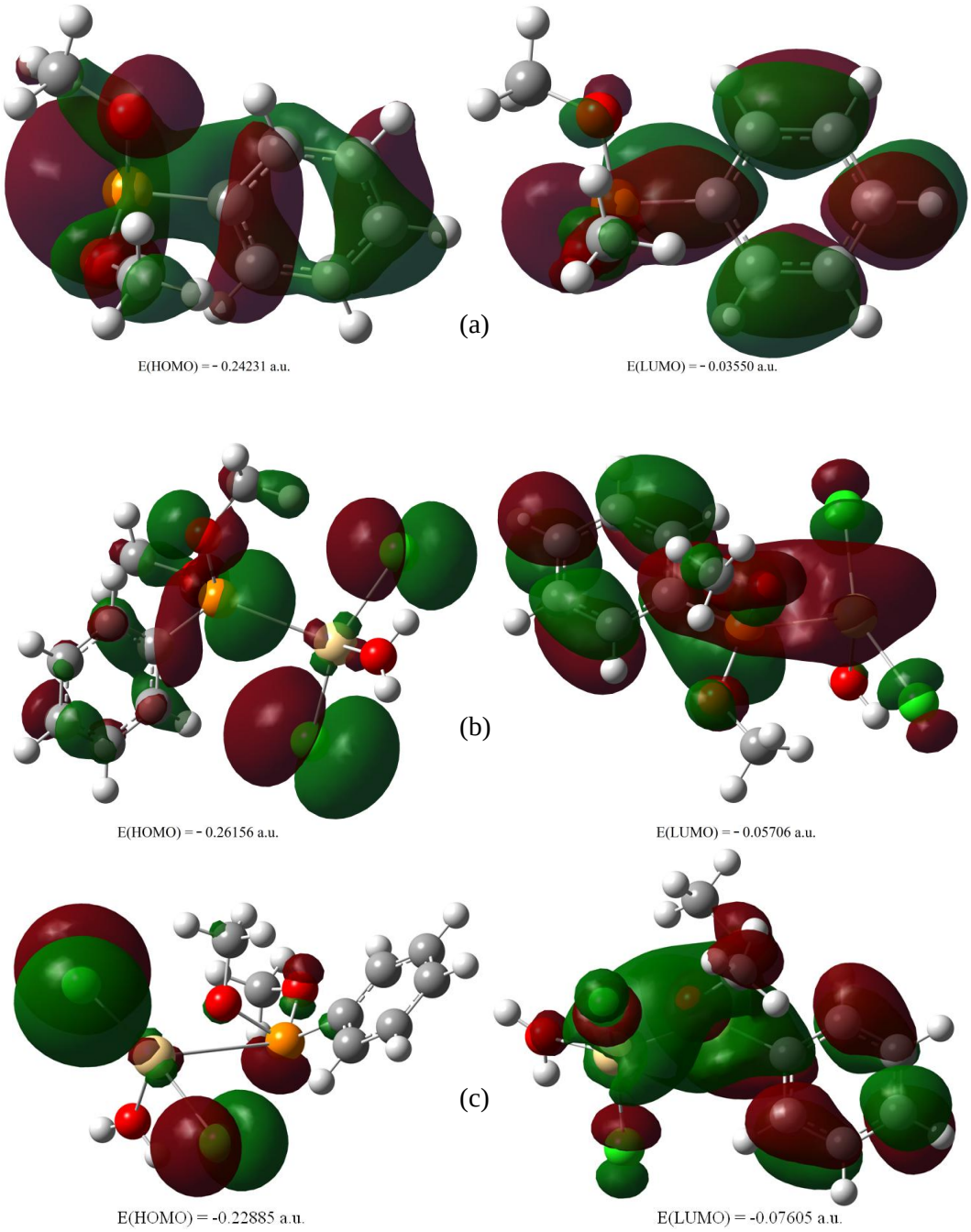

Figure 7. HOMO and LUMO plots of (a) free DMPP molecule at the B3LYP/6-311++G(d,p) level, (b) $Cd(DMPP)Cl_2.H_2O$ complex at the B3LYP/LanL2DZ level and (c) $Cd(DMPP)Cl_2.H_2O$ complex at the M06-L/LanL2DZ level

can be assigned to the ν(P-H) stretching mode in the metal complex [31,32]. The origin of these mentioned bands can be based on the increase in positive charge on phosphorus due to loss in P-O π-bonding and therefore the characteristically P-H stretching band is observed since the phosphorus is protonating in the formed complex [33]. Likewise by considering Table S3 and Figures 5 and 6, the band assigned to the ν(Cd-P) stretching vibration was not observed in the vibrational spectra of the mentioned

ISSN 2291-6458 (Print), ISSN 2291-6466 (Online)
Year 2014 | Volume 2 | Issue 2 | Page 175-189

metal halide complex, but the calculated value for this band was found as 90.11/ and 120.18 cm^{-1} at the B3LYP/LanL2DZ and M06-L/LanL2DZ levels, respectively. However the τ(HOCdP) torsion bands are observed at 283 cm^{-1} with very weak intensity and at 162 cm^{-1} with the weak intensity in the micro-Raman spectrum of the mentioned complex and their calculated values were found as 260.93/and 283.98 cm^{-1} and 130.14/and 189.16 cm^{-1} at the B3LYP/LanL2DZ and M06-L/LanL2DZ levels, respectively. Furthermore, the δ(ClCdO) bending mode is observed at 146 cm^{-1} with the weak intensity in micro-Raman spectrum of the mentioned complex and its calculated values was found as 110.36 and 146.14 cm^{-1} at the B3LYP/ LanL2DZ and M06-L/LanL2DZ levels, respectively. Likewise, the observed micro-Raman ν(Cd-P) stretching bands can be assigned to the weak band at 342 cm^{-1} and the peak at 256 cm^{-1} with very weak intensity [34] and the calculated values for these bands were found as 318.10 and 333.73 cm^{-1} and 245.77and 251.87 cm^{-1} as seen in Figure 6(a) and Table S3. By considering the observed results for the vibrational bands including Cd metal atom, a comparison between the calculated values using two different methods exhibits that the M06-L calculation method of the density functional theory gives better results than B3LYP method for the vibrational modes related to the Cd atom.

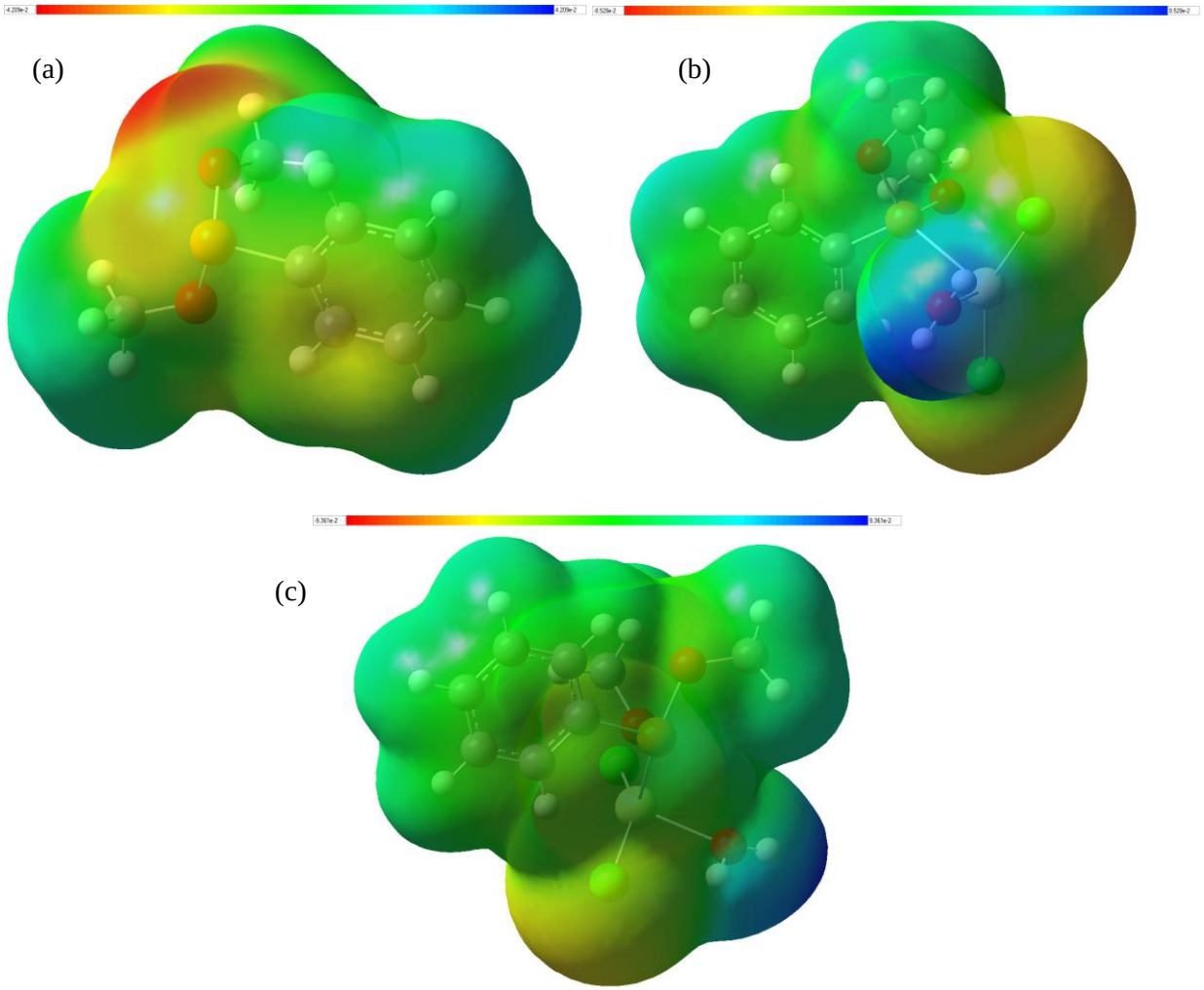

Figure 8. MEP surfaces of (a) free DMPP molecule at the B3LYP/6-311++G(d,p) level, (b) $Cd(DMPP)Cl_2.H_2O$ complex at the B3LYP/LanL2DZ level and (c) $Cd(DMPP)Cl_2.H_2O$ complex at the M06-L/LanL2DZ level (red negative and blue positive).

ISSN 2291-6458 (Print), ISSN 2291-6466 (Online)
Year 2014 | Volume 2 | Issue 2 | Page 175-189

4.2. Electronic Absorption and HOMO and LUMO Analysis

The observed electronic absorption spectral results of the mentioned compounds in dimethylformamide solvent show the maximum wavelength (λ_{max}) values at 278 nm (s) which can be attributed to the electronic $\pi \rightarrow \pi^*$ transition for free DMPP molecule and at 266 nm (vs) which can be assigned to the charge transfer (CT) transition of d^{10} system for $[Cd(C_8H_{11}PO_2)].Cl_2.H_2O$ complex [7]. On the other hand the highest occupied molecular orbital (HOMO) and the lowest unoccupied molecular orbital (LUMO) which are the main orbital taking part in chemical reactions of the molecules are called as the frontier molecule orbitals (FMOs) [35]. Therefore, the HOMO implies the outermost orbital filled by electrons and is directly related to the ionization potential and behaves as an electron donor while the LUMO can be thought as the first empty innermost orbital unfilled by electron and is directly related to the electron affinity and behaves as an electron acceptor. The energy gap formed between the HOMO-LUMO indicates the molecular chemical stability [35-36]. The energy gap between the HOMO-LUMO is a critical parameter to determine molecular electrical transport properties. The frontier molecular orbitals (FMOs) were calculated at the B3LYP/6-311++G(d,p) for free DMPP molecule and at the B3LYP/LanL2DZ and M06-L/LanL2DZ levels for $[Cd(DMPP)].Cl_2\ H_2O$ metal halide complex and the 3D plots and energy values of the HOMO-LUMO are given in Figure 7 (a), (b) and (c), respectively.

4.3 Molecular Electrostatic Potential (MEP)

The molecular electrostatic potential (MEP) which is related to total change distribution of the molecule provides the correlations between the molecular properties such as dipole moments, partial charges, chemical reactivity and electronegativity of molecules [37-38]. The molecular electrostatic potential is the potential energy of a proton at a particular location near a molecule. That is, the Molecular Electrostatic Potential (MEP), *V(r)*, at a given point *r(x,y,z)* in the around of molecule, is defined as the interaction energy between the charge distribution of a molecule and a unit positive test charge,

$$V(r) = \sum_A \frac{Z_A}{|R_A - r|} - \int \frac{\rho(r')}{|r' - r|} dr'$$

where Z_A denotes the charge of nucleus *A*, located at R_A distance, $\rho(r')$ denotes the charge density at point r', and r' is the dummy integration variable [38].

The 3D plots of the MEPs calculated from B3LYP/6-311++G(d,p) for free DMPP molecule and B3LYP/LanL2DZ and M06-L/LanL2DZ levels for the mentioned metal halide complex are exhibited in Figure 8 (a) and (b) and (c), respectively. Figures 8 show the electrostatic potentials at the surfaces which are represented by different colours for the mentioned compounds. Red and blue color parts represent the regions of negative and positive electrostatic potential, respectively, whereas green color parts represent the regions with zero potential. The negative regions of V(r) potential are related to electrophilic reactivity while positive ones are related to nucleophilic reactivity.

The negative sites on the MEP surface of free DMPP molecule given in Figure 8(a) are localized on the P and O atoms. Thus the coordination is expected to be formed in the electrophilic reactive sites on the mentioned atoms in the metal halide complex. Therefore, as seen in Table S1, since the calculated Cd-O10 bond length at the M06-L/LanL2DZ level was found shorter than the calculated Cd-P bond length the coordination is verified between O10 atom and Cd metal atom in the $[Cd(C_8H_{11}PO_2)].Cl_2.H_2O$ complex.

ISSN 2291-6458 (Print), ISSN 2291-6466 (Online)
Year 2014 | Volume 2 | Issue 2 | Page 175-189

5. CONCLUSION

In the present study, we report the results of elemental analysis, experimental vibrational and electronic absorption spectra of title compounds as well as their molecular geometries and the calculated vibrational spectral results at the B3LYP/6-311++G(d,p) level for free DMPP molecule and the B3LYP/LanL2DZ and M06-L/LanL2DZ levels of theory for $[Cd(C_8H_{11}PO_2)].Cl_2.H_2O$ metal halide complex. On the basis of the calculated and experimental results, the assignments of fundamental frequencies were investigated and the available experimental results were compared with the computed data. The calculations of vibrational frequencies and molecular electrostatic potentials on free and ligand DMPP enable us to predict the coordination between the one oxygen atom of methoxy groups of ligand DMPP molecule and the Cd(II) metal atom for tetrahedral $[Cd(C_8H_{11}PO_2)].Cl_2.H_2O$ complex.

ACKNOWLEDGEMENTS

This work was supported by Turkish Scientific and Technological Research Council (TÜBİTAK) (Project No: 111T6839) and Unit of Scientific Research Projects of Süleyman Demirel University (Project No: 3083-D-12).

SUPPORTING INFORMATION

Tables S1-S3 are included in the supporting information.

REFERENCES AND NOTES

[1] Ruggieri, R.; Hypodermic solutions of sodium dimethylphenylphosphonite and its methiodide derivative. *Giornale di Medicina Militare*, **1954**, *104 (3)*, 317-321.

[2] Birum, G. H. Triphosphinyl phospites. *US Patent Office*, **1961**, *3,014,945*, 1-10.

[3] Mrowca, J.J. Phosphinite, phosphonite, thiophosphinite and dithiophosphonite compounds of palladium and platinium. *US Patent Office*, **1973**, *3,776,929*, 1-10.

[4] Jenkins, J. M.; Moss, J. R.; Shaw, B. L. Substitute group VI metal carbonyl complexes with the ligand trimethylphosphine, dimethyl phenylphosphine, dimethyl phenylarsine and dimethyl phenylphosphonite. *J. Chem. Soc. A* **1969**, 2796-2800.

[5] Couch, D.A.; Robinson, S.D. Transition metal complexes containing phosphorous ligand. XII. Cationic dialkyl phenylphosphonite and alkyl diphenylphosphonite derivatives of copper, silver, gold and the platinium metals. *Inorg. Chem.* **1974**, *13*, 456-462.

[6] Sime, W. J.; Stephenson, T. A. Ruthenium complexes containing group 5B donor ligands. VI. Syntheses and rearrangement reactions of various $[RuCl_2L_{3\ or\ 4}]$ complexes [L = $P(OMe)_3$, $P(OMe)_2Ph$, P(OR) Ph_2 (R = Me, Et)]. *J. Organometal. Chem.* **1978**, *161*, 245-272.

[7] Mikulski, C. M.; Unruh, J.Ü; Pytlewski, L. L.; Karayannis, N. M. Methyl methylphenylphosphinate, MePh(MeO)PO complexes of the first row transition metals. *Trans. Met. Chem.* **1979**, *4*, 98-103.

[8] Brunner, H.; Jablonski, C. R.; Jones, P. G. Optically active transition metal compounds. Preparation, struvture, absolute configuration, and conformational analysis of chiral pseudoctahedral cobalt (III) phosphonato and phosphinato complexes. Optical induction in the transition-metal arbuzov reaction. *Organometallics*, **1998** *7*, 1283-1292.

[9] Kobeissi, M.; Simonneaux, G. ^{1}HNMR and EPR stud es of the electronic structure of low-spin iron (III) phosphonite mesotetraphenyl chlorine complexes: $a(d_{xy},d_{yz})^4(d_{xy})^1$. *Inorg. Chim. Acta*, **2003**, *343*, 18-26.

[10] Laing, M.; Reimann, R. H.; Singleton, E. Structure of five-coordinate di nitrosyls of manganase I. The monoclinic form of dinitrosylbis (dimethyl phenylphosphonite) manganase (I) chloride. Inorg.9 Chem.,

ISSN 2291-6458 (Print), ISSN 2291-6466 (Online)
Year 2014 | Volume 2 | Issue 2 | Page 175-189

1979, *18(2)*, 324-327.

[11] Laing, M; Reimann, R. H.; Singleton, E. Structures of five-coordinate dinitrosyls of manganese. 3. Dinitrosyltris(dimethyl phenylphosphonite)manganese(I) tetrafluoroborate, [Mn(NO)2{P(OCH3)2C6H5}3]BF4. *Inorg. Chem.* **1979**, *18(10)*, 2666-2670.

[12] Jablonski C R Ma H, Chen Z, Hynes R C, Bridson, J. N.; Bubenik, M. P. Diastreoselective arbusov dealkylation of cobalt (III) perfluoroalkyl prochiral phosphonite complexes. *Organometallics*, **1993**, *12(3)*, 917-926.

[13] Drust H. D.; Rohrbaugh, D. K.; Smith, P.; Niles, M. J.; Connell, T.; Laramee, J. A.; Munavalli, S. Anomalous reaction of ethyl bromofluoro- and difluoro-acetates with dialkylphosphonites. *Phosphorous, Sulfur and Silicon and the Related Elements*, **2008**, *183(11)*, 2655-2668.

[14] Slawin, A. M. Z.; Waddell, P. G.; Woolins, J. D. Cis-Dichloidobis (dimethoxyphenyl-phosphine) palladium (II). *Acta Cryst.*, **2010**, *E66*, m321.

[15] Slawin, A. M. Z.; Waddell, P. G.; Woolins, J. D. Cis-Dichloidobis (dimethoxyphenyl-phosphine) platinum (II).*Acta Cryst.*, **2010**, *E63*, m2017.

[16] Frisch, M. J. et al. *GAUSSIAN 09W: Re vision C. 01* (Wallingford, CT: Gaussian Inc.); 2009.

[17] Dennington, R.; Keith, T.; Millam, J. *GaussView; Version 5* (Shawnee Mission K S: Semichem Inc.); 2009.

[18] Becke, A. D. , Density-functional thermochemistry. III. The role of exact exchange . *J. Chem. Phys.* **1993**, *98*, 5648-5652.

[19] Lee, C.; Yang, W.; Parr, R. G. *Phys. Rev. B*, Development of the Colle-Salvetti correlation energy Formula into a functional of the electron density. **1988**, *37*, 785-789.

[20] Foresman, J. B.; Frish, E. *Exploring Chemistry with Electronic Structure Methods second edition* (Pittsburgh P A: Gaussian Inc.); 1996.

[21] Gökce, H.; Bahçeli, S. A study of molecular structure and vibrational spectra of copper (II) Halide complex of 2-(2'-thienyl)pyridine. *Spectroctrochim. Acta Part A*, **2012**, *96*, 139-147.

[22] Scott, A. P.; Radom, L. Harmonic vibrational frequencies: An evaluation of Hartree-Fock, Møller-Plesset, quadratic configuration interaction, density functional theory, and semiemprical scale factors. *J. Phys. Chem.*, **1996**, *100*, 16502-16513.

[23] Zhao, Y.; Truhlar, D. G. The M06 suite of density functionals for main group thermochemistry, thermochemical kinetics, noncovalent interactions, excited states, and transition elements: two new functionals and systematic testing of four M06-class functionals and 12 other functionals. *Theor. Chem. Account*, **2008**, *120 (1-3)*, 215-241.

[24] Cramer, C. J.; Truhlar, D. G. Density functional theory for transition metal chemistry. *Phys. Chem. Chem. Phys.*, **2009**, *11*, 10757-10816.

[25] Jonson, R. D. III (Ed.) *NIST Computational Chemistry Comparison and Benchmark Database, NIST Standart Reference Database* Number 101, Release 15b, August 2011.

[26] Jamr'oz, M. H. *Vibrational Energy Distribition Analysis: VEDA4* (Warsaw) 2004.

[27] Keresztury, G.; Holly, S.; Varga, J.; Besenyei, G.; Wang, A. Y.; Durig, J. R. Vibrational spectra of monothiocarbamates-II. IR and Raman spectra, vibrational assignment, conformational analysis and *ab initio* calculations of *S*-methyl-*N,N*-dimethylthiocarbamate. *Spectrochim. Acta. A*, **1993**, *49(13-14)*, 2007-2017.

[28] Keresztury, G., in: Chalmers J M and Griffith P R (Eds.), *Raman Spectroscopy: Theory in Hand book of Vibrational Spectroscopy* Vol. 1 (New York: John Wiley & Sons Ltd.), 2002.

[29] Bellamy, L., J 1975 *The Infrared Spectra of Complex Molecules* (3rd ed.) (New York: John Wiley &Sons, Inc.) Chapter 18.

[30] Colthup, N. B.; Lawrence, H. D.; Wiberley, S. E. *Introduction to Infrared and Raman Spectroscopy* (New York: Academic Pres) Chapter 12, p 298, 1964.

ISSN 2291-6458 (Print), ISSN 2291-6466 (Online)
Year 2014 | Volume 2 | Issue 2 | Page 175-189

[31] Stuart, B. H. *Infrared Spectroscopy: Fundamentals and Applications* (England: JohnWilley & Sons), 2004.
[32] Silverstein, R. M.; Webster, F. X. *Spectroscopic Identification of Organic Compound* (New York: John Willey & Sons), 1998.
[33] Verkade, J. G. Spectroscopic studies of metal-phosphorus bonding in coordination complexes. *Coordination Chemistry Reviews*, **1972**, 9 *(1)*, 1-106.
[34] Goel, R. G.; Ogini W. O. Preparation, characterization, and spectral studies of neutral tri-tert-butylphosphine complexes of zinc(II) and cadmium(II). *Inorg. Chem.*, **1977**, 16, 1968- 1972.
[35] Fukui, K. Role of Frontier Orbitals in Chemical Reactions. *Science*, **1982**, *218*, 747-754.
[36] Pearson, R. G. Absolute electronegativity and hardness correlated with molecular orbital theory. *Proc. Natl. Acad. Sci. USA*, **1986**, *83*, 8440-8441.
[37] Pirnau, A.; Chiş, V.; Oniga, O.; Leopold, N.; Szabo, L.; Baias, M.; Cozar, O. Vibrational and DFT study of 5-(3-pyridyl-methylidene)-thiazolidine-2-thione-4-one *Vib. Spectrosc*. **2008**, *48(2)*, 289-296.
[38] Murray, J. S.; Sen, K. *Molecular Electrostatic Potentials Concepts and Applications* (Amsterdam, The Netherlands: Elsevier Science B.V.), 1996.

The authors declare no conflict of interest

© 2014 By the Authors; Licensee Borderless Science Publishing, Canada. This is an open access article distributed under the terms and conditions of the Creative Commons Attribution license http://creativecommons.org/licenses/by/3.0/